

# Annealing ambient controlled deep defect formation in InP

Y. W. Zhao<sup>1,a</sup>, Z. Y. Dong<sup>1</sup>, M. L. Duan<sup>1</sup>, W. R. Sun<sup>1</sup>, Y. P. Zeng<sup>1</sup>, N. F. Sun<sup>2</sup>, and T. N. Sun<sup>2</sup>

<sup>1</sup> Materials Science Centre, Institute of Semiconductors, Chinese Academy of Science, PO Box 912, Beijing 100083, P.R. China

<sup>2</sup> Hebei Semiconductor Research Institute, PO Box 179, Shijiazhuang 050051, Hebei, P.R. China

Received: 2 July 2003 / Accepted: 9 December 2003 – © EDP Sciences

**Abstract.** Deep defects in annealed InP have been investigated by deep level transient capacitance spectroscopy (DLTS), photo induced current spectroscopy (PICTS) and thermally stimulated current spectroscopy (TSC). Both DLTS results of annealed semiconducting InP and PICTS and TSC results of annealed semi-insulating InP indicate that InP annealed in phosphorus ambient has five defects, while InP annealed in iron phosphide ambient has two defects. Such a defect formation phenomenon is explained in terms of defect suppression by the iron atom diffusion process. The correlation of the defects and the nature of the defects in annealed InP are discussed based on the results.

**PACS.** 61.72.Ji Point defects (vacancies, interstitials, color centers, etc.) and defect clusters – 81.05.Ea III-V semiconductors – 71.55.Eq III-V semiconductors

## 1 Introduction

InP has become an important material for the fabrication of optoelectronic and microwave devices used in the modern communication systems. Defects in InP can be created in the processes of growth [1,2], thermal annealing [3], etc. In recent years, high temperature thermal annealing has become a useful method to improve the electrical uniformity [4], reduce the residual thermal stress [5] and to obtain low Fe content semi-insulating material [6–9]. In this paper, we present experimental results of deep level defects in InP annealed in phosphorus and iron phosphide ambients. Defect formation phenomena related with the in-diffusion of iron and phosphorus atom have been studied.

## 2 Experiment

The samples used in the experiment were prepared by annealing n type undoped InP wafers grown by liquid encapsulated Czochralski (LEC) method. The electron concentration of the as-grown LEC undoped InP was  $(3\text{--}12)\times 10^{15}\text{ cm}^{-3}$ . The annealing was carried out in a sealed quartz tube at 930 °C for 80 hours. A quantity of 6N's red phosphorus or 5N's Fe powder and 6N's red phosphorus at a mole ratio of 1:2 was charged in the quartz

tube before annealing. In this way, pure phosphorus (PP) or iron phosphide (IP) with moderate vapor pressure can be formed at the annealing temperature [10,11] and Fe diffusion was thus realized. After annealing the wafers were cooled at 40 °C/h to room temperature. This process was found to convert the undoped n type LEC InP with carrier concentration below  $6 \times 10^{15}\text{ cm}^{-3}$  to a SI material with resistivity and mobility above  $10^7\ \Omega\cdot\text{cm}$  and  $(3000\text{--}4200)\text{ cm}^2/\text{V}\cdot\text{s}$ , respectively. The SI InP wafer so formed exhibits good profile and radial uniformity [12]. It should be mentioned that undoped LEC InP with a carrier concentration below  $3 \times 10^{15}\text{ cm}^{-3}$  can also be annealed into SI material under similar conditions, the only difference of which being that the ambience in the quartz tube is pure phosphorus. After annealing, as-grown undoped InP with carrier concentration of  $1.2 \times 10^{16}\text{ cm}^{-3}$  still semiconducting is used as sample for deep level transient spectroscopy (DLTS) study. As-grown Fe-doped SI InP samples have also been studied by thermally stimulated current spectroscopy (TSC) and photo-induced current transient spectroscopy (PICTS).

Samples with a size of  $3 \times 8 \times 0.6\text{ mm}^3$  were used for the TSC and PICTS measurements. A layer of more than 60  $\mu\text{m}$  of the SI InP wafer was removed during the lapping and polishing process. Electrical parameters of the samples were measured by the conventional Hall effect method. Alloyed indium was used to make ohmic contact for the measurements. The conditions of the TSC measurement are: applied bias 10 V, heating rate 0.3 K/s and initiated light illumination by an 850 nm LED at a power of 50 mW for 10 minutes.

<sup>a</sup> e-mail: zhaoyw@red.semi.ac.cn

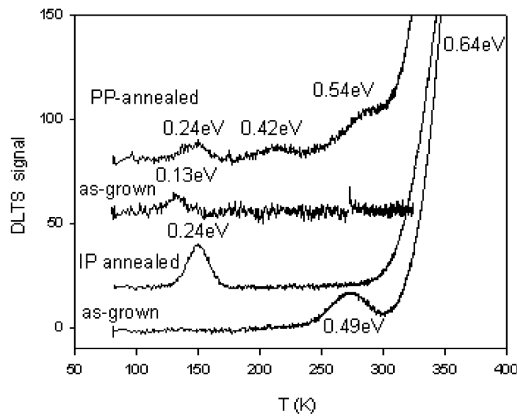


**Fig. 1.** DLTS spectra of as-grown and annealed undoped InP samples.

## 3 Results

### 3.1 DLTS of annealed semiconducting InP

Defects in annealed semiconducting InP have been studied by DLTS, the results are shown in Figure 1. Two defects at 0.49 eV and 0.64 eV are detected in an as-grown InP sample and only one defect at 0.13 eV is observed in another sample. The 0.64 eV defect is the well-known Fe acceptor in InP, incorporated as residual impurity contamination. The origins of the 0.49 eV and 0.13 eV defects are not clear. They are most likely native defects in as-grown InP. This will be further evidenced by comparison with the defects in annealed InP. In the phosphorus ambient annealed InP, four defects at 0.24 eV, 0.42 eV, 0.54 eV and 0.64 eV have been detected, while two defects at 0.24 eV and 0.64 eV were observed in the sample annealed in iron phosphide ambient. An obvious fact is that Fe diffusion suppresses the formation of the two defects at 0.42 eV and 0.54 eV that are formed in phosphorus in-diffusion process.

### 3.2 TSC of annealed SI InP

TSC spectra of the annealed SI InP and as-grown Fe-doped SI InP are shown in Figure 2. The energy levels of deep defects in the SI InP samples can be obtained by the approximation formula:  $E_T = kT_m \ln(T_m^4/\beta)$ , where  $k$  is the Boltzman constant,  $T_m$  is the peak temperature,  $\beta$  is the heating rate. Defect levels at 0.18 eV, 0.22 eV, 0.26 eV, 0.32 eV, 0.37 eV and 0.48 eV are identified in an IP-SI-InP. In the PP-SI-InP, the deep level defects are at 0.18 eV, 0.26 eV, 0.37 eV, 0.45 eV and 0.48 eV. In two as-grown Fe-doped SI InP samples, deep defects at 0.22 eV, 0.27 eV, 0.32 eV, 0.37 eV are observed in one sample and two levels at 0.18 eV, 0.24 eV in another one. The IP-SI InP has much lower concentration of the defects than the PP-SI InP and as-grown Fe-doped SI InP. These defects are not observed in two IP-SI InP samples.

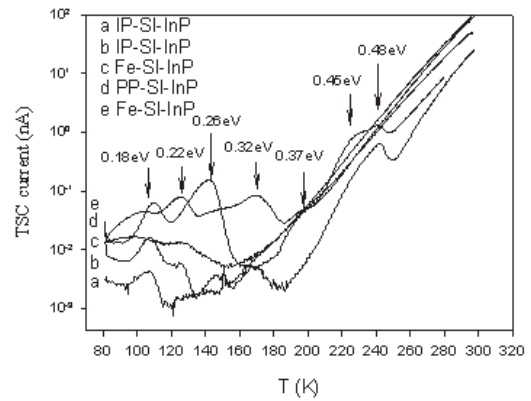


**Fig. 2.** TSC spectra of Fe-doped and annealed undoped SI InP samples.

### 3.3 PICTS of annealed SI InP

PICTS spectra of an IP-SI InP and a PP-SI InP are shown in Figure 3. A phenomenon similar to the TSC spectra is

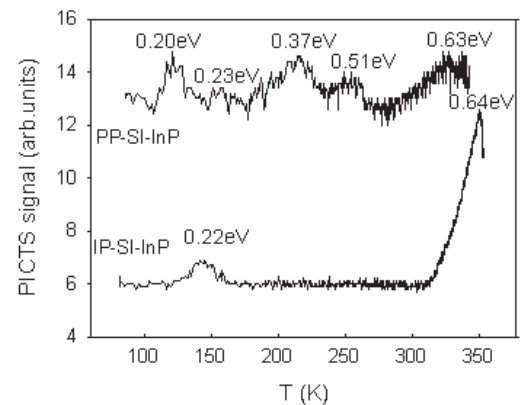


**Fig. 3.** PICTS spectra of a PP annealed and an IP annealed SI InP samples.

observed. Except the Fe acceptor deep level at 0.64 eV, there is only one defect at 0.22 eV in the IP-SI InP, while four defects at 0.20 eV, 0.23 eV, 0.37 eV, 0.51 eV are found in the PP-SI InP. Although TSC detects more defects in the same IP-SI InP due to a higher sensitivity of the technique, the concentrations of the defects are very low ( $10^{12} \text{ cm}^{-3}$ ). Therefore, the PICTS result is basically consistent with the result of TSC, indicating a defect suppression phenomenon of Fe diffusion once again.

## 4 Discussion

The results of DLTS, TSC and PICTS consistently indicate a phenomenon of defect suppression by Fe diffusion. Since the primary difference of PP and IP annealing is the diffusion species involved, the defect formation and suppression must be related to the diffusion atom. It is

apparently that only in-diffusion of phosphorus atom exists in the PP annealing process, while in-diffusion of both phosphorus and iron atoms proceed in the IP annealing process. It has to be considered that iron atom diffuses faster than phosphorus atom in InP [13]. It is also known that the Fe atom occupies the indium site and acts as a deep acceptor in InP [14]. Based on these facts, it is reasonable to think that the defects suppressed by the Fe diffusion are related with indium vacancy. Since the occupation of the indium site by phosphorus atom results in the formation of antisite defect, one of the defects at 0.42 eV observed in PP-InP can be assigned to a phosphorus antisite defect. This is in agreement with the results of InP annealed in phosphorus ambient in which the concentration of a defect at 0.42 eV increases with the increasing of ambient pressure [15].

The 0.24 eV defect has been found in both PP and IP annealed InP, its concentration increases after IP annealing. It is most likely a defect complex with Fe or deep level impurity such as Mn [16] incorporated in the annealing processes. It is noted that the 0.42 eV defect and the 0.54 eV defect can be suppressed by the Fe diffusion simultaneously, indicating their intrinsic nature. We assign the 0.54 eV defect to a complex defect related with phosphorus antisite. The two defects have not been detected in as-grown Fe-doped SI InP. Two defects at 0.26 eV and 0.32 eV, which are also suppressed by the Fe diffusion, are very probably related with indium vacancy. The existence of indium vacancy with considerable concentration in as-grown InP has been confirmed by positron annihilation experiment [17, 18].

## 5 Conclusion

After high temperature annealing in PP and IP ambient, undoped InP samples exhibit different defect formation behavior. In the IP annealing process, Fe diffusion suppresses the formation of some defects. On the contrary, pure phosphorus diffusion enhances the formation of these defects in the PP annealing process.

## References

1. S. H. Chiao, G. A. Antypas, *J. Appl. Phys.* **49**, 466 (1978)
2. T. Temkin, B. V. Dutt, W. A. Bonner, *Appl. Phys. Lett.* **38**, 431 (1981)
3. H. J. von Bardeleben, D. Stievenard, K. Kainosho, O. Oda, *J. Appl. Phys.* **70**, 7392 (1991)
4. M. Avella, J. Jimenez, A. Alvarez, R. Fornari, E. Gilioli, A. Sentiri, *J. Appl. Phys.* **82**, 3836 (1997)
5. Masayuki Fukuzawa, Martin Herms, Masayuki Uchida, Osamu Oda, Masayoshi Yamada, *Jpn. J. Appl. Phys.* **38**, 1156 (1999)
6. D. Hofmann, G. Müller, N. Streckfuss, *Appl. Phys. A* **48**, 315 (1989)
7. K. Kainosho, H. Shimakura, H. Yamamoto, O. Oda, *Appl. Phys. Lett.* **59**, 932 (1991)
8. R. Fomari, A. Zappettini, E. Gombia, R. Mosca, K. Cherkaoui, G. Marrakchi, *J. Appl. Phys.* **81**, 7604 (1997)
9. M. Uchida, T. Asahi, K. Kainosho, Y. Matsuda, O. Oda, *Jpn. J. Appl. Phys.* **38**, 986 (1999)
10. D. Wolf, G. Hirt, G. Müller, *J. Electron. Mater.* **24**, 933 (1995)
11. Y. W. Zhao, H. W. Dong, Y. H. Chen, Y. H. Zhang, J. H. Jiao, J. Q. Zhao, L. Y. Lin, S. Fung, *Appl. Phys. Lett.* **80**, 2878 (2002)
12. Y. W. Zhao, H. W. Dong, J. H. Jiao, J. Q. Zhao, L. Y. Lin, N. F. Sun, T. N. Sun, *Chinese J. Semicon.* **23**, 285 (2002)
13. P. Kipfer, J. Lindolf, D. Hofmann, G. Müller, *J. Appl. Phys.* **69**, 3860 (1993)
14. S. Fung, R. J. Nicholas, R. A. Stradling, *J. Phys. C: Solid State Phys.* **12**, 5145 (1979)
15. G. Marrakchi, K. Cherkaoui, A. Karoui, G. Hirt, G. Müller, *J. Appl. Phys.* **79**, 6947 (1996)
16. M. S. Skolnick, E. J. Foulkes, B. Tucck, *J. Appl. Phys.* **55**, 2951 (1984)
17. T. Bretagon, S. Dannefaer, D. Kerr, *J. Appl. Phys.* **73**, 4697 (1997)
18. C. Corbel, C. Leberre, K. Saarinen, P. Hautajarvi, *Mater. Sci. Eng. B* **44**, 173 (1997)